European Journal of Obstetrics & Gynecology and Reproductive Biology 171 (2013) 301–306

Contents lists available at ScienceDirect

European Journal of Obstetrics & Gynecology and Reproductive Biology

journal homepage: www.elsevier.com/locate/ejogrb

Effect of HSP10 on apoptosis induced by testosterone in cultured mouse ovarian granulosa cells

Kao-Kao Zhao [a], Yu-Gui Cui [a,*], Ya-Qin Jiang [b], Jing Wang [a], Mei Li [a], Yuan Zhang [a], Xiang Ma [a], Fei-Yang Diao [a], Jia-Yin Liu [a]

[a] State Key Laboratory of Reproductive Medicine, Clinical Centre of Reproductive Medicine, First Affiliated Hospital, Nanjing Medical University, Nanjing, China
[b] Maternal and Child Health Hospital in Changzhou, Jiangsu, China

ARTICLE INFO

Article history:
Received 17 February 2013
Received in revised form 12 July 2013
Accepted 22 September 2013

Keywords:
HSP10
Apoptosis
Granulosa cells
Polycystic ovarian syndrome

ABSTRACT

Objective: To investigate the effect of heat shock protein 10 (HSP10) on apoptosis induced by testosterone in granulosa cells (GCs) of mouse ovaries in order to define the possible roles of HSP10 in ovarian pathological development of polycystic ovarian syndrome (PCOS) and hyperandrogenic conditions.

Study design: Cultured mouse ovarian GCs were treated with testosterone (10^{-5} mol/l). Apoptosis was assessed using flow cytometry, and proliferation was assessed using the MTT assay. HSP10 expression in the treated GCs was detected by real-time polymerase chain reaction (PCR). *HSP10* gene was downregulated in the cultured GCs by AdCMV-H1-SiRNA/HSP10 or overexpressed by AdCMV-HSP10. PD98059 [phosphorylated ERK (p-ERK) inhibitor] was used to treat GCs to induce a high apoptosis index. Critical apoptotic factors and proliferation factors, including P-ERK, Bcl-2, Bax, caspase 9, caspase 3 and Ki67, were monitored by real-time reverse transcriptase PCR (RT-PCR) and Western blot.

Results: Compared with the control group, the apoptosis index was higher ($p < 0.05$) and HSP10 expression was lower ($p < 0.05$) in the testosterone-treated groups. In the AdCMV-H1-SiRNA/HSP10-treated group, cell viability was decreased ($p < 0.05$) and the cell cycle was arrested at G2. Expression of p-ERK, Bcl-2 and Ki67, and the Bcl-2:Bax ratio were lower, while expression of apoptotic factors, including Bax, caspase 9 and caspase 3, was higher ($p < 0.05$). Compared with the control group, Bcl-2 expression in the GCs that overexpressed HSP10 was increased ($p < 0.05$), while the reduction of p-ERK and Bcl-2 and the elevation of caspase 9 and caspase 3 induced by PD98059 were significantly suppressed ($p < 0.05$).

Conclusions: Hyperandrogenic conditions induced apoptosis of mouse GCs. Testosterone may have reduced HSP10 expression in GCs, leading to reduced Bcl-2 expression and increased Bax expression.

1. Introduction

HSP10 is an important member of the heat shock protein (HSP) family [1]. It plays a role in cell protection, and inhibits cell apoptosis by regulating the key signaling pathways of apoptosis. Shan et al. found that doxorubicin induced myocardial cell injury, and HSP10 reduced this injury *via* the mitochondria apoptosis pathway, upregulating Bcl-2 and downregulating Bax [2]. HSP10 protects muscle cells from damage by hydrogen peroxide, sodium cyanide and ischemia reperfusion through the Ras-Raf-ERK pathway [3]. The expression of HSPs, such as HSP10, is significantly increased in the ischemic brain [4]. The increased expression of HSP10 protects myocardial cells from ischemia-reperfusion injury by reducing the release of cytc and inhibiting the activation of caspase 3 [5]. Schlieper et al. found that HSP10 was one of the important anti-apoptosis factors in ventricular myocytes [6]. Recently, many studies have found that HSP10 expression is significantly increased in tumor tissues, such as colorectal cancer, cervical cancer, prostate cancer and lymphoma, which may be related to its anti-apoptotic functions [7–10].

In the ovaries of patients with polycystic ovarian syndrome (PCOS), characterized by chronic anovulation, hyperandrogenism

* Corresponding author at: Centre of Clinical Reproductive Medicine, Department of Obstetrics and Gynaecology, First Affiliated Hospital of Nanjing Medical University, 300 Guangzhou Road, Nanjing, Jiangsu Province, Nanjing 210029, China. Tel.: +86 25 86862288; fax: +86 25 86862288.
E-mail address: cuiygnj@njmu.edu.cn (Y.-G. Cui).

0301-2115/$ – see front matter © 2013 Elsevier Ireland Ltd. All rights reserved.
http://dx.doi.org/10.1016/j.ejogrb.2013.09.026

and polycystic changes [11–14], there is an imbalance between pro-apoptosis and anti-apoptosis in ovarian granulosa cells (GCs). It has been reported that GC apoptosis in PCOS is closely related to the hyperandrogenic condition. GC apoptosis has been shown to be increased in various PCOS animal models induced by androgens. However, the mutual causality has not been clarified to date. A previous study by the present authors showed that HSP10 expression was lower in ovarian GCs from PCOS patients compared with those from normal women [15–17]. This study investigated the role of HSP10 in regulating apoptosis of mouse GCs induced by testosterone in order to further define the possible role of HSP10 in the ovarian pathological development of PCOS and hyperandrogenic conditions.

2. Materials and methods

2.1. Materials

Rabbit anti-ERK peptide polyclonal antibody, rabbit anti-phosphorylated-ERK (p-ERK) peptide polyclonal antibody and PD98059 (p-ERK inhibitor) were purchased from Cell Signaling Technology (Danvers, MA, USA). DMEM/F12 was purchased from Hyclone Co. (Logan, UT, USA), and hyaluronidase and fetal bovine serum (FBS) were purchased from Sigma Chemical Co. (St Louis, MO, USA). Antibiotic–antimycotic preparations (penicillin 10,000 IU/ml, streptomycin 10,000 mg/ml) were purchased from Grand Island Biological Co. (New York, NY, USA). TRIZOL reagent was purchased from Invitrogen (Carsbad, CA, USA). All other reagents were purchased from Sigma–Aldrich (St Louis, MO, USA). AdCMV-H1-small interfering RNA (SiRNA)/HSP10 and AdCMV-HSP10 were constructed by the study group in previous work [17].

2.2. Mouse ovarian granulosa cells cultured in vitro

Ovaries of immature PMSG-treated mice were cleaned of surrounding connective tissue and placed into DMEM/F12 supplemented with 5% FBS, glutamine (2 mmol/l), penicillin (100 units/ml) and streptomycin (100 g/ml) [17]. GCs were harvested by ovarian follicle puncture with a needle. Cells were recovered by centrifugation at 300 × *g* for 10 min, washed twice, inoculated into six- or 96-well culture dishes at a density of 5×10^5 cells/ml, and cultured at 37 °C in a humidified atmosphere of 95% air and 5% CO_2.

2.3. MTT analysis to assess cell viability

MTT assays were used to assess the viability of mouse GCs as follows: 0, 10^{-8}, 10^{-6} and 10^{-5} mol/l testosterone-treated groups; and AdH1-null and AdH1-siRNA/HS10-infected groups. Forty-eight hours later, 20 μl fresh MTT reagent (5 μg/μl) was added to each well and the cells were cultured at 37 °C in 5% CO_2 for another 4 h. The medium was discarded carefully, and 150 μl DMSO was added and vortexed for 10 min. The absorbance value was measured on a microplate reader (Bio-Rad) at 560 nm. Assays were performed in triplicate and data were expressed as mean ± standard deviation (SD).

2.4. Flow cytometry analysis to detect apoptosis and cell cycle

Mouse ovarian GCs (5×10^5 cells) were cultured. After reaching 70% confluence, the cells were treated with 10^{-5} mol/l testosterone. Menstruum was used as the control (0 mol/l testosterone). Forty-eight hours later, cells were harvested by 0.25% trypsinization, washed with PBS, centrifuged at 800 revolutions/min for 5 min and the supernatant was removed. FITC-conjugated annexin V (0.5 μg/ml final concentration) and propidium iodide (PI, 1 μg/ml final concentration) were added according to the manufacturer's instructions (Beijing Biosea Biotechnology Co., Ltd., Beijing, China). After incubation for 20 min at room temperature, 400 μl binding buffer was added, and the samples were analyzed immediately on a FACS Sort Flow Cytometer (Becton Dickinson and Company, Mountainview, CA, USA) with excitation at 488 nm using an excitation wave argon ion laser. PI was added to samples to distinguish necrotic and late apoptotic events (annexin V−, PI+; annexin V+, PI+) from early apoptotic events (annexin V+, PI−).

The cell cycle phase was assayed by DNA fragment staining using PI. A Cell Cycle Phase Determination Kit (Cayman Chemical, Ann Arbor, MI, USA) was used according to the manufacturer's protocol. Mouse GCs (5×10^5 cells) were cultured. After reaching 70% confluence, the cells were infected with AdCMV-H1-SiRNA/HSP10 or AdCMV-H1-SiRNA/control. Forty-eight hours later, cells were harvested by 0.25% trypsinization, washed with PBS, fixed with cold 75% ethanol overnight, and stored at −20 °C pending cell cycle analysis. Prior to cell cycle analysis, cells were resuspended in PBS containing RNase A (20 μg/ml, Sigma) and 20 μg/ml PI (Sigma), and incubated at 37 °C for 30 min before analysis for PI fluorescence intensity with the FACS Sort Flow Cytometer (Becton Dickinson and Company).

2.5. Western blot assay of ERK and p-ERK

The GCs infected with AdCMV-H1-SiRNA/HSP10, AdCMV-H1-SiRNA/control, AdCMV-HSP10 or AdCMV (control) for 48 h were collected. A phosphorylated protein extraction kit (Sigma–Aldrich) was used to extract protein. Total proteins were extracted and separated by SDS–PAGE, and transferred on to a polyvinylidene difluoride membrane (GE Healthcare, San Francisco, CA, USA). Following transfer, the membranes were blocked in Tris-buffered saline (TBS) containing 5% bovine serum albumin (Sigma–Aldrich) for 1 h at room temperature, and then incubated overnight with anti-ERK or anti-p-ERK antibodies (1:1000) at 4 °C. After washing three times in TBS for 10 min each time, membranes were incubated for 1 h at 37 °C with horseradish-peroxidase-conjugated secondary antibody (1:1000; Zhongshan Biotechnology Co. Ltd., Beijing, China), washed three times, and then examined by enhanced chemiluminescence (Amersham Biosciences, Uppsala, Sweden). The membranes were subsequently scanned, and the signal intensity of each band was determined using AlphaEaseFC (Fluorchem 5500) software (Alpha Innotech Corp., San Leandro, CA, USA).

2.6. Real-time RT-PCR analysis of Ki67, Bcl-2, Bax, caspase 9 and caspase 3

Real-time RT-PCR was performed for quantitative assessment of mRNA expression of the proliferation- and apoptosis-related factors, including Ki67, Bcl-2, Bax, caspase 9 and caspase 3. The cells infected with AdCMV-H1-SiRNA/HSP10, AdCMV-H1-SiRNA/control, AdCMV-HSP10 or AdCMV (control cells) were harvested. Total RNA was extracted using TRIZOL reagent. The extracted RNA was measured by spectrometry at $OD_{260/280}$, and equal amounts of RNA (50 ng) were reverse transcribed into cDNA. The sequences of primers used for real-time RT-PCR assessment of Ki67, Bcl-2, Bax, caspase 9 and caspase 3 expression are listed in Table 1. Each sample was assayed in duplicate using the equivalent of 1 μl cDNA, 10 pmol primer and 1 μl SYBR Green Master Mix (Applied Biosystems, Foster City, CA, USA) in a total reaction volume of 20 μl. For normalization purposes, an identical set of reactions was prepared using specific primers for β-actin or GAPDH mRNAs. Amplification was performed in an ABI Prism 7300 Sequence Detection System (PerkinElmer, Applied Biosystems) as follows: 50 °C/2 min, 95 °C/10 s (1×); and 95 °C/5 s, 60 °C/30 s (40×).

Table 1
Primers used for real-time reverse transcriptase polymerase chain reaction.

Gene	Primer[a]	Sequence	Size (bp)
HSP10	Forward Reverse	GGGAGATCTATGGCTGGACAAGCTTTTAG GGGCTCGAGTCAGTCGACATACTTTCCAA	309
Ki67	Forward Reverse	CCTCTTGGTTGGCGTTTC CCTGGTCTTAGTTCCGTTGA	278
Bcl-2	Forward Reverse	TCGCCCTGTGGATGACTGA CACTTGTGGCCCAGGTATG	202
Bax	Forward Reverse	GGCGAATTGGAGATGAACTG CAAAGTAGAAGAGGGCAACCAC	236
Caspase 3	Forward Reverse	ATGGGAGCAAGTCAGTGGAC CGTACCAGAGCGAGATGACA	137
Caspase 9	Forward Reverse	GGCGGAGCTCATGATGTCTGTG TTCCGGTGTGCCATCTCCATCA	269
GAPDH	Forward Reverse	AGGTTGTCTCCTGCGACTTCA GGGTGGTCCAGGGTTTCTTACT	216
Beta-actin	Forward Reverse	GAGACCTTCAACACCCCAGC ATGTCACGCACGATTTCCC	263

[a] Sequences are from 5 to 3, ends.

Melting curve analysis was performed to confirm the real-time RT-PCR products. Relative abundance of the target mRNAs was calculated with the $2^{-\Delta\Delta CT}$ method [18].

2.7. Statistical analysis

Data were expressed as mean ± SD from at least three independent experiments. Student's *t*-test was used for statistical comparison. *p* values <0.05 were considered significant.

3. Results

3.1. Apoptosis of mouse ovarian GCs induced by testosterone

MTT analysis showed that the viability of mouse GCs in the groups treated with 10^{-6} and 10^{-5} mol/l testosterone were significantly lower compared with the control group ($p < 0.05$) (Fig. 1A). Flow cytometry analysis showed that the percentage of apoptotic GCs in the group treated with 10^{-5} mol/l testosterone was significantly higher (38.53%) than that in the control group (28.36%) ($p < 0.05$) (Fig. 1B).

3.2. HSP10 expression in GCs treated with testosterone

To detect the effect of testosterone on HSP10 expression in GCs, the cultured GCs were treated with 0, 10^{-8}, 10^{-6} and 10^{-5} mol/l testosterone. Real-time RT-PCR showed that HSP10 expression was significantly downregulated by treatment with 10^{-6} and 10^{-5} mol/l testosterone compared with the control group ($p < 0.05$), and HSP10 expression in the group treated with 10^{-5} M testosterone was lower than that in the group treated with 10^{-6} M testosterone ($p < 0.05$) (Fig. 2).

3.3. Proliferation in mouse GCs treated with SiRNA/HSP10

HSP10 expression in mouse GCs was reduced by adenovirus-delivered SiRNA; the interference efficiency of SiRNA/HSP10 was approximately 70% (Fig. 3A). Cell viability in the SiRNA/HSP10 group was significantly lower compared with the control group ($p < 0.05$) (Fig. 3B), while the cell cycle was arrested at G_2 in the SiRNA/HSP10 group (Fig. 3C).

3.4. Anti-apoptotic factors and pro-apoptotic factors were differentially regulated in mouse GCs treated with SiRNA/HSP10

The anti-apoptosis factors p-ERK (Fig. 4A), Bcl-2 (Fig. 5A) and Ki67 (Fig. 5D) were downregulated, whereas the pro-apoptosis

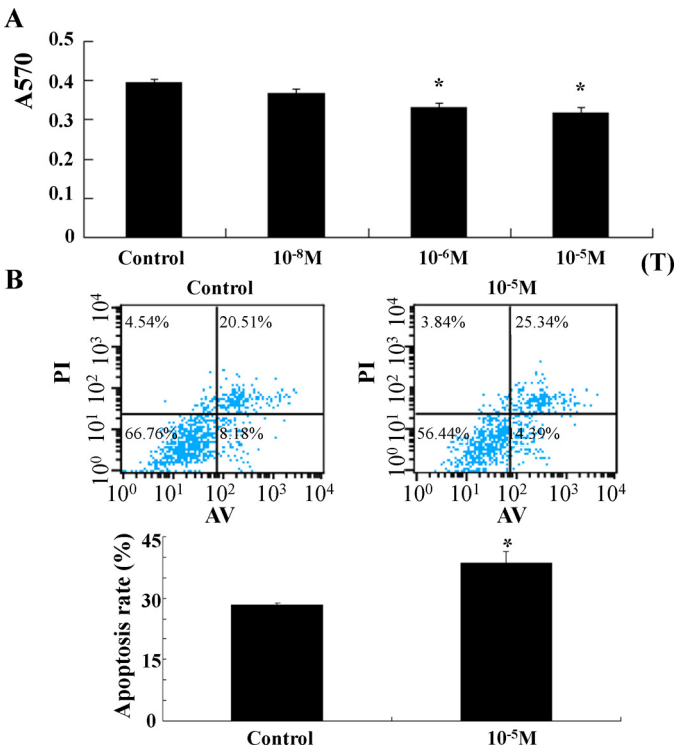

Fig. 1. Apoptosis of mouse granulosa cells (GCs) treated with testosterone was detected by MTT and flow cytometry analysis. (A) GCs were treated with 0, 10^{-8}, 10^{-6} and 10^{-5} M testosterone. Cell viability was detected by MTT analysis. Values were presented as mean ± standard deviation. $^{*}p < 0.05$ was found in the 10^{-6} M and 10^{-5} M testosterone-treated groups compared with the control group. (B) GCs were treated with 0 and 10^{-5} M testosterone, apoptosis was detected by flow cytometry analysis. The apoptotic rate in the 10^{-5} M testosterone-treated group (38.53%) was higher than that in the control group (28.36%, $^{*}p < 0.05$). T, testosterone; PI, propidium iodide.

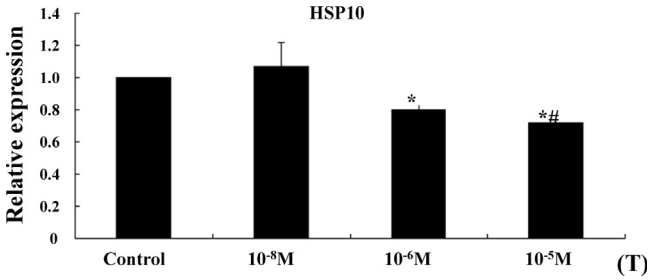

Fig. 2. HSP10 expression in mouse granulosa cells (GCs) treated with testosterone was detected by real-time reverse transcriptase polymerase chain reaction. GCs were treated with 0, 10^{-8} M, 10^{-6} M and 10^{-5} M testosterone. Values were presented as mean ± standard deviation. $^{*}p < 0.05$ was found in the 10^{-6} M and 10^{-5} M testosterone-treated groups compared with the control group. $\#p < 0.05$ was found in the 10^{-5} M testosterone-treated group compared with the 10^{-6} M testosterone-treated group.

factors Bax (Fig. 5B), caspase 9 (Fig. 5E) and caspase 3 (Fig. 5F) were upregulated, and the Bcl-2:Bax ratio was significantly decreased (Fig. 5C) in the siRNA/HSP10 group compared with the control group ($p < 0.05$). This indicated the anti-apoptotic role of HSP10 in mouse GCs.

3.5. Overexpression of HSP10 suppressed the apoptotic effect of PD98059 in mouse GCs

To determine the best effective concentration of PD98059 as an inhibitor of p-ERK, mouse GCs were treated with 0, 20, 50 and 100 μmol/l PD98059 for 1 h. As 50 μmol/l of PD98059 was found to be the best inhibitory concentration, it was selected for the following tests (Fig. 4B). To further determine the anti-apoptotic role of HSP10 in mouse GCs, qPCR was used to analyze the expression of the anti-apoptosis factor Bcl-2 and the pro-apotosis factors caspase 9 and caspase 3 in mouse GCs treated with PD98059 and PD98059 plus AdCMV-HSP10. Bcl-2 expression was significantly decreased in the PD98059 group compared with the control group, whereas Bcl-2 expression was relatively elevated when HSP10 was overexpressed (Fig. 6A). Expression of the pro-apoptosis factors caspase 9 and caspase 3 was significantly

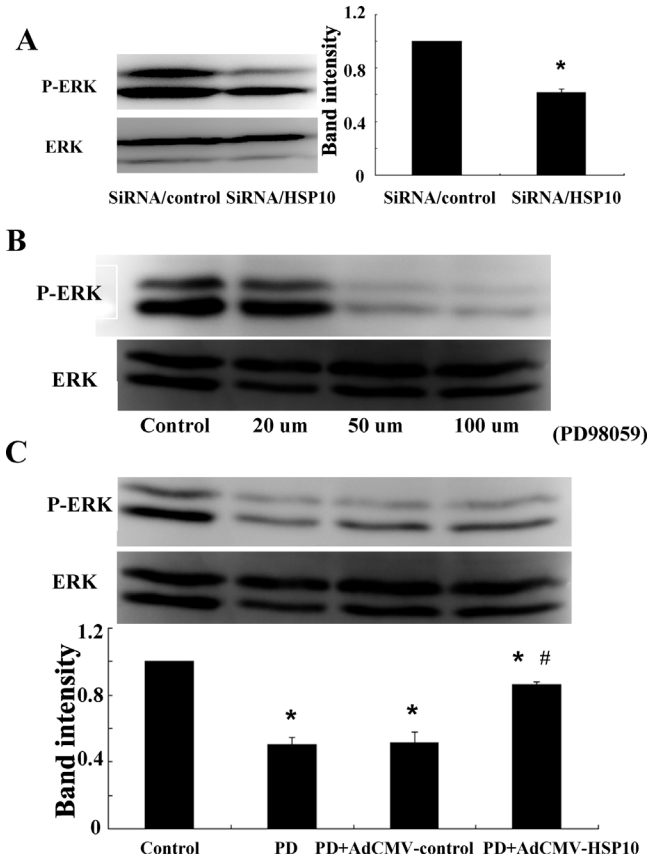

Fig. 4. Expression of phosphorylated-ERK (p-ERK) was detected by Western blot analysis. (A) Expression of p-ERK was reduced in the SiRNA/HSP10 group compared with the control group ($^{*}p < 0.05$). (B) Expression of p-ERK in mouse granulosa cells (GCs) treated with PD98059 (p-ERK inhibitor). GCs were treated with 50 and 100 μM PD98059 for 1 h. Expression of p-ERK in two PD98059-treated groups was decreased. (C) HSP10 had an inhibitory effect on PD98059-induced apoptosis. GCs were infected by AdCMV-HSP10 and AdCMV-control for 48 h, then treated with 50 μM PD98059 for 1 h. $^{*}p < 0.05$ was found in the PD98059 group, PD98059 + AdCMV-control group and PD98059 + AdCMV-HSP10 group compared with the control group. $\#p < 0.05$ was found in the PD98059 + AdCMV-HSP10 group compared with the PD98059 + AdCMV-control group. Values were presented as mean ± standard deviation.

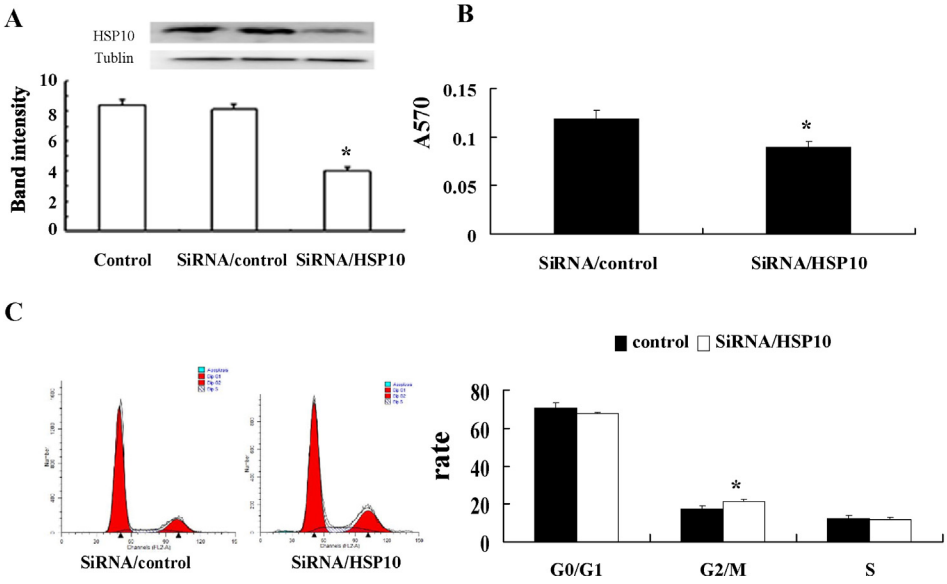

Fig. 3. Cell viability and cell cycle in mouse granulosa cells (GCs) infected with AdCMV-H1-SiRNA/HSP10. (A) Interference efficiency of AdCMV-H1-siRNA/HSP10 in mouse GCs. (B) Cell viability was detected by MTT analysis. Cell viability was lower in the siRNA/HSP10 group compared with the control group. (C) Cell cycle was detected by flow cytometry analysis. The cell cycle was arrested at G2 after reducing HSP10 expression. Values were presented as mean ± standard deviation. $^{*}p < 0.05$ was found in the siRNA/HSP10 group compared with the control group.

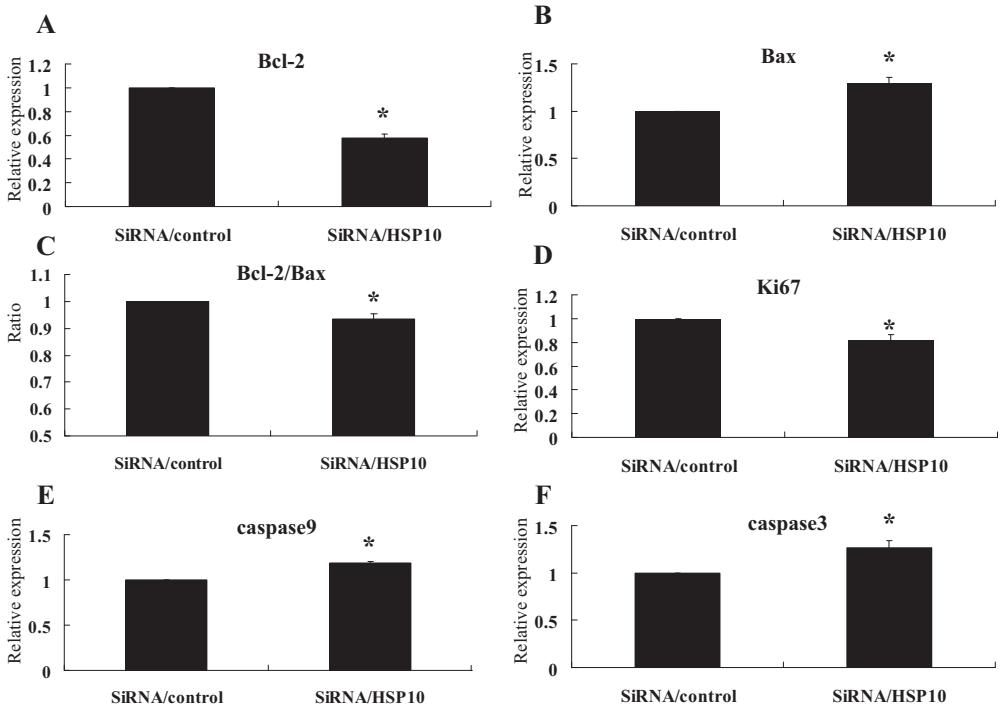

Fig. 5. Apoptosis-related factors were detected by real-time reverse transcriptase polymerase chain reaction in mouse granulosa cells infected with AdCMV-H1-SiRNA/HSP10. Expression of anti-apoptosis factors such as Bcl-2 (A) and Ki67 (D) was decreased, while the expression of pro-apoptosis factors such as Bax (B), caspase 9 (E) and caspase 3 (F) was increased, and the Bcl-2:Bax ratio was decreased in the SiRNA/HSP10 group compared with the SiRNA/HSP10 group. Values were presented as mean ± standard deviation. $^{*}p < 0.05$ was found in the SiRNA/HSP10 groups compared with the control group.

increased in the PD98059 group, and decreased in the HSP10 overexpression group (Fig. 6B and C).

3.6. Comments

There is an imbalance between apoptosis and anti-apoptosis in the ovaries of women with PCOS. The expression of apoptosis-related factors in PCOS ovaries is higher compared with normal ovaries [19], and the expression of PDCD5, a novel apoptosis-related protein, is higher in the GCs of PCOS ovaries compared with the control group [20]. Recent studies found that apoptosis of GCs was increased in the DHEA-induced PCOS rat model along with the imbalance of Bcl-2 family members: Bcl-2 protein decreased and Bax protein increased [21]. Meanwhile, it has been reported that the expression of apoptosis factors such as TRAIL, Fas, FasL and membrane type 1-matrix metalloproteinase is increased in ovarian GCs of hyperandrogen-induced PCOS rats [22,23]. Thus, it was hypothesized that GC apoptosis might be closely related to hyperandrogenism, and that GC apoptosis is involved in the pathological development of PCOS. In this study, mouse GCs were cultured *in vitro*. Cell viability was lower and the apoptotic rate was higher in the testosterone-treated groups compared with the control group.

HSP10, an important member of the HSP family, was involved in regulation of signal transduction such as cell proliferation, differentiation and apoptosis. The authors' previous studies showed that HSP10 was expressed in all follicular cell types, and that HSP10 expression was downregulated in human GCs of PCOS ovaries [16]. In another study, the authors found that HSP10 was only expressed in mouse oocytes of antral follicles, while HSP10 was expressed in oocytes, GCs and theca cells after culture [24]. It was concluded that downregulation of HSP10 expression in GCs of PCOS ovaries was responsible for the increased apoptosis of GCs, and thus affected follicular development. Previous studies also found that the apoptosis index was increased in mouse GCs transfected with the recombinant mouse HSP10-SiRNA [17]. This study found that HSP10 expression was decreased in mouse GCs treated with testosterone, and that cell viability was lowered and the cell cycle was arrested at G_2 in mouse GCs infected with AdCMV-H1-SiRNA/HSP10.

This series of studies suggested that HSP10 is a downstream factor in ovarian GC apoptosis induced by testosterone. However, its detailed mechanism of action is still unclear. ERK1 and ERK2 are co-expressed in all mammalian tissues and implicated as key regulators of cell proliferation and differentiation, as well as oocyte maturation *in vitro* [25,26]. The Erk1$^{-/-}$and Erk2$^{gc-/-}$ females were fertile; however, the Erk1/2$^{gc-/-}$ females failed to ovulate and were completely infertile. In Erk1/2$^{gc-/-}$ females, no oocytes matured, no cumulus cell-oocyte complex expanded, GCs exhibited signs of apoptosis and luteinization failed [15]. In this study, the lowered HSP10 expression by adenoviral infection reduced the expression of p-ERK, while HSP10 overexpression attenuated the effect of the ERK inhibitor (PD98059). ERK regulated apoptosis through regulation of the Bcl-2 family proteins [27]. In this study, the lower expression of HSP10 regulated the expression of Bcl-2 family proteins by upregulating the pro-apoptosis factor Bax and down-regulating the anti-apoptosis factor Bcl-2, thus decreasing the Bcl-2:Bax ratio, along with upregulating the downstream pro-apoptotic factors caspase 9 and caspase 3. This effect was the same as that of PD98059, an ERK inhibitor. Overexpression of HSP10 inhibited the effect induced by PD98059. Thus, HSP10, acting as a downstream factor in the process of GC apoptosis induced by testosterone, may function by downregulating the expression of p-ERK, thus mediating mitochondrial apoptotic pathways by affecting the expression of Bcl-2 family proteins.

In conclusion, HSP10 was found to regulate testosterone-induced apoptosis of mouse GCs through the ERK and mitochondrial apoptosis pathways. However, the specific actions between

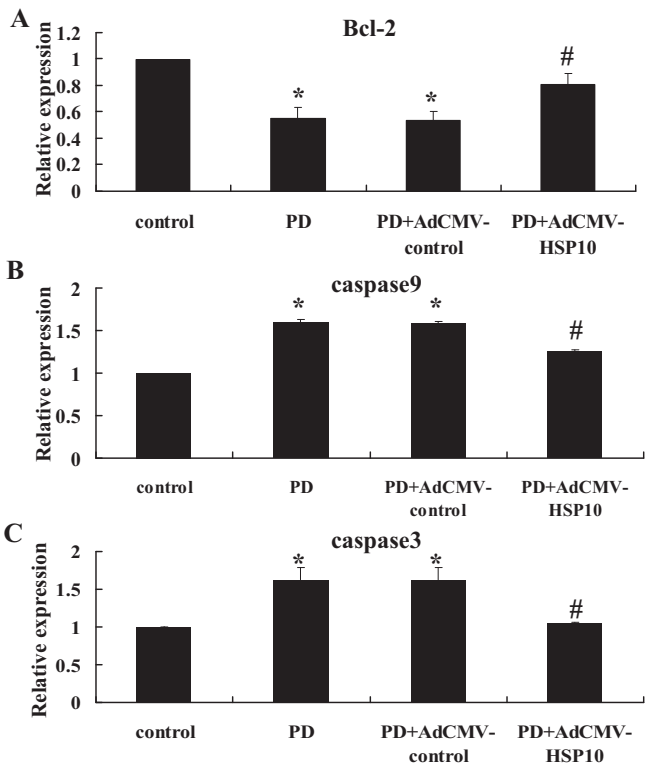

Fig. 6. Apoptosis-related factors were detected by real-time reverse transcriptase polymerase chain reaction in mouse granulosa cells infected with AdCMV-HSP10 and treated with PD98059. (A) Expression of anti-apoptosis factors such as Bcl-2 was decreased in the PD98059-treated groups compared with the control group, while overexpression of HSP10 inhibited this downregulation. Expression of pro-apoptosis factors such as caspase 9 (B) and caspase 3 (C) was increased in the PD98059-treated groups compared with the control group, while overexpression of HSP10 inhibited this upregulation. $^{*}p < 0.05$ was found in the PD98059-treated group and PD98059 + AdCMV-control group compared with the control group. $\#p < 0.05$ was found in the PD98059 + AdCMV-HSP10 group compared with the PD98059 + AdCMV control group. Values were presented as mean ± standard deviation.

hyperandrogenism and HSP10 need further study. HSP10 may affect the development and maturation of oocytes and follicles in the pathological process of hyperandrogenism in PCOS. As the oocyte maturation rate, fertilization rate, cleavage rate and high-quality embryo formation rate were closely associated with the apoptotic rate of GCs in PCOS patients [28,29], HSP10 may be a potential research target for the pathophysiological mechanism of PCOS.

Conflict of interest

None declared.

Acknowledgements

This work was supported by projects from China 973 Program (2012CB944703, 2012CB944902) and a project from Jiangsu Changzhou (CS2008223), China. This work was also supported by the Priority Academic Program Development of Jiangsu Higher Education Institutions.

References

[1] Feder ME, Hofmann GE. Heat-shock proteins, molecular chaperones, and the stress response: evolutionary and ecological physiology. Annu Rev Physiol 1999;61:243–82.
[2] Shan YX, Liu TJ, Su HF, Samsamshariat A, Mestril R, Wang PH. Hsp10 and Hsp60 modulate Bcl-2 family and mitochondria apoptosis signaling induced by doxorubicin in cardiac muscle cells. J Mol Cell Cardiol 2003;35:1135–43.
[3] Lin KM, Hollander JM, Kao VY, Lin B, Macpherson L, Dillmann WH. Myocyte protection by 10 kDa heat shock protein (Hsp10) involves the mobile loop and attenuation of the Ras GTP-ase pathway. FASEB J 2004;18:1004–6.
[4] Izaki K, Kinouchi H, Watanabe K, et al. Induction of mitochondrial heat shock protein 60 and 10 mRNAs following transient focal cerebral ischemia in the rat. Brain Res Mol Brain Res 2001;88:14–25.
[5] Lin KM, Lin B, Lian IY, Mestril R, Scheffler IE, Dillmann WH. Combined and individual mitochondrial HSP60 and HSP10 expression in cardiac myocytes protects mitochondrial function and prevents apoptotic cell deaths induced by simulated ischemia-reoxygenation. Circulation 2001;103:1787–92.
[6] Schlieper A, Anwar M, Heger J, Piper HM, Euler G. Repression of anti-apoptotic genes via AP-1 as a mechanism of apoptosis induction in ventricular cardiomyocytes. Pflugers Arch 2007;454:53–61.
[7] Cappello F, Bellafiore M, David S, Anzalone R, Zummo G. Ten kilodalton heat shock protein (HSP10) is overexpressed during carcinogenesis of large bowel and uterine exocervix. Cancer Lett 2003;196:35–41.
[8] Cappello F, Rappa F, David S, Anzalone R, Zummo G. Immunohistochemical evaluation of PCNA, p53, HSP60, HSP10 and MUC-2 presence and expression in prostate carcinogenesis. Anticancer Res 2003;23:1325–31.
[9] Cappello F, David S, Rappa F, et al. The expression of HSP60 and HSP10 in large bowel carcinomas with lymph node metastase. BMC Cancer 2005;5:139.
[10] Ghobrial IM, McCormick DJ, Kaufmann SH, et al. Proteomic analysis of mantle-cell lymphoma by protein microarray. Blood 2005;105:3722–30.
[11] Knochenhauer ES, Key TJ, Kahsar-Miller M, Waggoner W, Boots LR, Azziz R. Prevalence of the polycystic ovary syndrome in unselected black and white women of the southeastern United States: a prospective study. J Clin Endocrinol Metab 1998;83:3078–82.
[12] Sengoku K, Tamate K, Takuma N, Yoshida T, Goishi K, Ishikawa M. The chromosomal normality of unfertilized oocytes from patients with polycystic ovarian syndrome. Hum Reprod 1997;12:474–7.
[13] Diamanti-Kandarakis E, Kouli CR, Bergiele AT, et al. A survey of the polycystic ovary syndrome in the Greek island of Lesbos: hormonal and metabolic profile. J Clin Endocrinol Metab 1999;84:4006–11.
[14] Asuncion M, Calvo RM, San Millan JL, Sancho J, Avila S, Escobar-Morreale HF. A prospective study of the prevalence of the polycystic ovary syndrome in unselected Caucasian women from Spain. J Clin Endocrinol Metab 2000;85:2434–8.
[15] Fan HY, Liu Z, Shimada M, et al. MAPK3/1 (ERK1/2) in ovarian granulosa cells are essential for female fertility. Science 2009;324:938–41.
[16] Ma X, Fan L, Meng Y, et al. Proteomic analysis of human ovaries from normal and polycystic ovarian syndrome. Mol Hum Reprod 2007;13:527–35.
[17] Ling J, Zhao KK, Cui YG, et al. Heat shock protein 10 regulated apoptosis of mouse ovarian granulosa cells. Gynecol Endocrinol 2011;27:63–71.
[18] Livak KJ, Schmittgen TD. Analysis of relative gene expression data using real-time quantitative PCR and the 2(−Delta Delta C(T)) method. Methods 2001;25:402–8.
[19] Jansen E, Laven JS, Dommerholt HB, et al. Abnormal gene expression profiles in human ovaries from polycystic ovary syndrome patients. Mol Endocrinol 2004;18:3050–63.
[20] Sun CL, Qiao J, Hu ZX, Zhang T, Chen YY. Expression of novel apoptosis-related protein PDCD5 in granulosa cells of polysystic ovary syndrome. Beijing Da Xue Xue Bao 2005;37:476–9.
[21] Bas D, Abramovich D, Hernandez F, Tesone M. Altered expression of Bcl-2 and Bax in follicles within dehydroepiandrosterone-induced polycystic ovaries in rats. Cell Biol Int 2011;35:423–9.
[22] Zhang J, Zhu G, Wang X, Xu B, Hu L. Apoptosis and expression of protein TRAIL in granulosa cells of rats with polycystic ovarian syndrome. J Huazhong Univ Sci Technol Med Sci 2007;27:311–4.
[23] Honnma H, Endo T, Henmi H, et al. Altered expression of Fas/Fas ligand/caspase 8 and membrane type 1-matrix metalloproteinase in atretic follicles within dehydroepiandrosterone-induced polycystic ovaries in rats. Apoptosis 2006;11:1525–33.
[24] Fan L, Ling J, Ma X, Cui YG, Liu JY. Involvement of HSP10 during the ovarian follicular development of polycystic ovary syndrome: study in both human ovaries and cultured mouse follicles. Gynecol Endocrinol 2009;25:392–7.
[25] Su YQ, Wigglesworth K, Pendola FL, O'Brien MJ, Eppig JJ. Mitogen-activated protein kinase activity in cumulus cells is essential for gonadotropin-induced oocyte meiotic resumption and cumulus expansion in the mouse. Endocrinology 2002;143:2221–32.
[26] Chen Z, Gibson TB, Robinson F, et al. MAP kinases. Chem Rev 2001;101:2449–76.
[27] Yang ZH, Sun K, Suo WH, et al. N-stearoyltyrosine protects primary neurons from a beta-induced apoptosis through modulating mitogen-activated protein kinase activity. Neuroscience 2010;169:1840–7.
[28] Liu S, Jiang JJ, Feng HL, Ma SY, Li M, Li Y. Evaluation of the immature human oocytes from unstimulated cycles in polycystic ovary syndrome patients using a novel scoring system. Fertil Steril 2010;93:2202–9.
[29] Filali M, Frydman N, Belot MP, et al. Oocyte in-vitro maturation: BCL2 mRNA content in cumulus cells reflects oocyte competency. Reprod Biomed Online 2009;19:4309.